

Quark structure of the pion and pion form factor

V. Anisovich,* D. Melikhov,† and V. Nikonov

St. Petersburg Institute of Nuclear Physics, Gatchina 188350, Russia

(Received 24 March 1995)

We consider the pion structure in the region of low and moderately high momentum transfers: at low Q^2 , the pion is treated as a composite system of constituent quarks; at moderately high momentum transfers, $Q^2 = 10\text{--}25 \text{ GeV}^2$, the pion form factor is calculated within perturbative QCD taking into account one-gluon hard exchange. Using the data on the pion form factor at $Q^2 < 3 \text{ GeV}^2$ and the pion axial-vector decay constant, we reconstruct the pion wave function in the soft and intermediate regions. This very wave function combined with the one-gluon hard scattering amplitude allows a calculation of the pion form factor in the hard region $Q^2 = 10\text{--}25 \text{ GeV}^2$. A specific feature of the reconstructed pion wave function is a quasizone character of the $q\bar{q}$ excitations. On the basis of the obtained pion wave function and the data on deep inelastic scattering off the pion, the valence quark distribution in a constituent quark is determined.

PACS number(s): 12.39.-x, 11.55.Fv, 12.38.Bx, 14.40.Aq

I. INTRODUCTION

Perturbative QCD (PQCD) gives rigorous predictions for exclusive amplitudes, in particular, form factors at asymptotically large values of Q^2 [1]. For the pion form factor defined as

$$\langle \pi(P') | J_\beta | \pi(P) \rangle = (P' + P)_\beta F_\pi(Q^2), \quad (1)$$

the PQCD result takes the form

$$F_\pi(Q^2) = 8\pi f_\pi^2 \frac{\alpha_s(Q^2)}{Q^2} \left[1 + \sum_{N=2,4,\dots} C_N \left(\ln \frac{Q^2}{\mu^2} \right)^{-\gamma_N} \right] + O(1/Q^4). \quad (2)$$

Here γ_N are the known positive numbers calculated within PQCD, μ is a constant about 1 GeV dividing the perturbative and nonperturbative regions, $f_\pi = 130 \text{ MeV}$ is the pion axial-vector decay constant, and the C_N are expressed through the soft-region nonperturbative wave function of the pion. In the series (2), the contribution of diagrams with internal lines having virtualities above μ are taken into account perturbatively, while all the exchanges with lower virtualities are absorbed into the set of soft nonperturbative wave functions of the pion Fock components. The terms of order $1/Q^2$ come only from the valence quark-antiquark component of the pion Fock state, whereas other components give the terms $O(1/Q^4)$. The series (2) involves both the leading and subleading logarithms. In the leading logarithmic approximation (LLA) the expression (2) can be rewritten in the form

$$F_\pi(Q^2) = \int_0^1 dx dx' \phi_\pi(x, Q^2) T_B(x, x', Q^2) \phi_\pi(x', Q^2), \quad (3)$$

where $\phi(x, Q^2)$ is the leading twist wave function (distribution amplitude) which describes the longitudinal momentum distribution of valence quark-antiquark pair whose relative transverse momentum is less than Q and

$$T_B(x, x', Q^2) \rightarrow \frac{8\pi \alpha_s(x x' Q^2)}{9 x x' Q^2} \quad (4)$$

is the amplitude of the hard interaction of the two free quarks in the Born approximation [Fig. 1(a)].

The distribution amplitude at large Q is related to the soft pion distribution amplitude $\phi_\pi(x, \mu^2)$ by the gluon ladder evolution kernel $K(x, y, Q^2/\mu^2)$ as follows:

$$\phi_\pi(x, Q^2) = \int K(x, y, Q^2/\mu^2) \phi_\pi(y, \mu^2) dy. \quad (5)$$

The soft distribution amplitude is connected with the pion axial-vector decay constant via the relation

$$\int \phi_\pi(x, \mu^2) dx = f_\pi, \quad f_\pi = 130 \text{ MeV}. \quad (6)$$

So in the LLA, hard scattering off the pion described by expressions (3) and (5) [see Fig. 1(b)] has a clear physical interpretation within the hard scattering picture [2]: namely, the initial pion transforms into a quark-antiquark pair with a small relative transverse momentum $\leq \mu$ and the longitudinal momentum fractions x and $1-x$, respectively; this stage is described by $\phi(y, \mu^2)$. Next, the quarks are coming closer to each other at a distance of $1/Q$ and increase their virtualities via ladder gluon exchanges, described by K . Then, the hard interaction of almost free quarks with the external current occurs (T_B), and inverse evolution occurs to low virtualities (K) with a subsequent pion formation [$\phi(y', \mu^2)$]. A rigorous QCD result is that any soft distribution ampli-

*Electronic address: anisovic@lnpi.spb.su

†Also at Nuclear Physics Institute, Moscow State University. Electronic address: melikhov@npi.msu.su

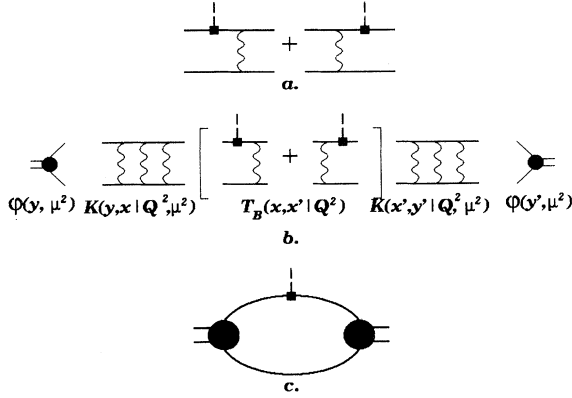


FIG. 1. (a) Hard scattering amplitude for two free quarks in the Born approximation. (b) Hard scattering process in the LLA. (c) Soft form factor.

tude evolves at large Q^2 to the universal function

$$\phi_\pi^{\text{as}}(x) = \phi_\pi(x, Q^2 \rightarrow \infty) = 6f_\pi x(1-x). \quad (7)$$

Substituted into (3), this function gives the leading term in (2).

Unfortunately, this beautiful picture does not work at momentum transfers accessible to present-day experiments: The momentum transfers are not large enough. Trying to adjust this perturbative calculations for moderately high momentum transfers, Chernyak and Zhitnitsky [3] assumed the logarithmic and power corrections (including a purely soft contribution shown in Fig. 1) to the Born term not to be essential, and the pion form factor to be described by

$$F_\pi(Q^2) = \int_0^1 dx \phi_\pi(x, \mu^2) T_B(x, x', Q^2) dx' \phi_\pi(x', \mu^2), \quad (8)$$

with T_B still given by (4), but with some modified distribution amplitude ϕ_π . Describing the available pion form factor data by formula (8), they came to the soft distribution amplitude of the form

$$\phi_\pi^{\text{CZ}}(x, \mu \approx 0.5 \text{ GeV}) = 30f_\pi x(1-x)(1-2x)^2. \quad (9)$$

However, arguments against such an approach were put forward by Isgur and Llewellyn-Smith [4]. The problem is that the wave function of the form (9) strongly emphasizes the end-point region of $x \approx 0$ which was estimated to give 70–90% of pion form factor at $Q^2 = 10 \text{ GeV}^2$. Recall that only the exchanges with virtualities above μ^2 were considered perturbatively; otherwise the corresponding subprocesses were referred to the soft wave function. In the end-point region at moderately high Q^2 , the gluon virtuality $xx'Q^2$ is not large enough to justify the perturbative treatment. Hence, the end-point contribution should be rather referred to the nonperturbative one. The large contribution coming from small x means

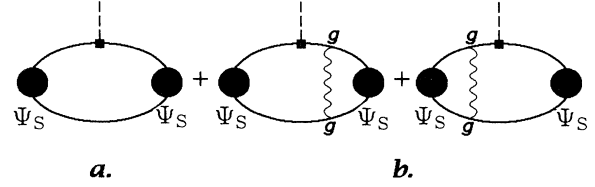


FIG. 2. The expansion of the pion form factor in the series over g^2 .

that in fact the wave function with strongly emphasized end points has picked up a good portion of the nonperturbative contribution. So the latter turns out not to be small, which contradicts the initial assumption.

The arguments of [4] were supported by recent applications of QCD sum rules [5,6]: The end-point contribution remains numerically important at least up to $Q^2 \approx 10 \text{ GeV}^2$, although parametrically it is suppressed by an extra power of $1/Q^2$. The problem of a correct extraction of the end-point contribution to hard scattering amplitudes was studied by Li and Sterman [7] and Radyushkin [8]. Their results give additional arguments against the application of the strategy of Ref. [3] to hadron form factors at intermediate momentum transfers.

In addition, some problems are encountered when wave functions with an emphasized end-point region are applied to deep inelastic scattering. It was discussed [9] that the valence quark contribution to the deep inelastic structure function calculated with such distribution amplitudes exceeds the available data at large x , whereas there should be a room for other Fock components.

Attempts to describe the pion form factor in the region $Q^2 = 3\text{--}10 \text{ GeV}^2$ taking into account only the perturbative hard scattering mechanism were not successful. The nonperturbative contribution in this region is obviously not small. Our goal is to consider the pion form factor at moderately large Q^2 , allowing for both perturbative and nonperturbative contributions starting with low Q^2 and advancing to higher values.

Investigations of soft hadron processes in past decades have demonstrated constituent quarks to be relevant objects for describing hadron structure [10,11].

The nonperturbative contribution to the pion form factor was considered within the framework of a QCD-inspired constituent quark model [12–16], the pion form factor being represented by the diagram of Fig. 1(c).

In the approach suggested here, we move to the region of large Q^2 starting with small values. That is, we take into account the diagram of Fig. 2(a) and, as the following step, the diagrams of Fig. 2(b). The diagrams of Fig. 2(b) correspond to terms with a minimal $N = 0$ in the series (2). In fact, we recast the series (2) for the pion form factor as a series over α_s . Such an expansion is relevant at moderately large Q^2 .

To be more quantitative, the procedure is as follows. The expansion for the pion form factor in a series over α_s reads

$$J^\beta(0) = [\bar{q}(0)\gamma^\beta q(0)]_{\mu^2} + \alpha_s \int dz_1 dz_2 [\bar{q}(0)q(z_1)]_{\mu^2} \langle 0 | T_B^\beta(z_1, z_2) \langle 0 | [\bar{q}(z_2)q(0)]_{\mu^2} + O(\alpha_s^2). \quad (10)$$

To make this expansion meaningful, the operator product expansion was performed; i.e., all the field operators were decomposed into soft and hard components. The subscript μ^2 implies that the subdiagrams for the corresponding operators involve only lines with virtualities below μ^2 . The contribution of the region of virtualities below μ^2 is described by the soft wave functions, whereas the contribution of larger virtualities is represented by the hard scattering block T_B [1].

Let us denote the corresponding contributions of the first and second terms in the right-hand side (RHS) of (10) as F^{SS} [Fig. 2(a)] and $2F^{SH}$ [Fig. 2(b)], respectively. Then one finds

$$F_\pi = F^{SS} + 2F^{SH} + O(\alpha_s^2). \quad (11)$$

The last series actually corresponds to dividing the pion light-cone wave function Ψ into two parts such that Ψ_S is large at $s = \frac{m^2}{x(1-x)} < s_0$ while Ψ_H prevails at $s > s_0$. We perform such a decomposition of the wave function using the simplest ansatz with the step function:

$$\Psi = \Psi_S \theta(s_0 - s) + \Psi_H \theta(s - s_0). \quad (12)$$

According to (10), Ψ_H is represented as a convolution of the one-gluon exchange kernel V^{α_s} with Ψ_S :

$$\Psi_H = V^{\alpha_s} \otimes \Psi_S. \quad (13)$$

The soft-soft contribution F^{SS} in (11) is the usual quantity calculated within constituent quark models, whereas the soft-hard term F^{SH} relates to the one given by the hard scattering mechanism. The soft-soft contribution includes the Sudakov form factor of the quark. We obtain the following results.

(i) The pion form factor calculated in the region of Q^2 from 0 to 20 GeV^2 describes well the available data (Fig. 3). The soft-soft contribution is found to give more than one-half of the form factor in the region $Q^2 \leq 20 \text{ GeV}^2$ (Fig. 4) and is not negligible up to $Q^2 \leq 30 \text{ GeV}^2$. However, the particular numbers depend on how we define the boundary of the soft and the hard regions. We assume an extended soft region for $s \leq 9 \text{ GeV}^2$ that yields a large contribution of the soft-soft form factor until very high momentum transfers.

The transverse motion in the soft-hard term turns out to be important. At the same time, the Sudakov suppression is not large in the kinematical region of momentum transfers where the soft-soft term dominates.

(ii) The soft pion wave function which has been a variational quantity of our consideration is found to have a quasizone structure: It is large at low $s \leq 2 \text{ GeV}^2$, then it almost vanishes at $2 \text{ GeV}^2 \leq s \leq 4.5 \text{ GeV}^2$, and has a bump at $4.5 \text{ GeV}^2 \leq s \leq 9 \text{ GeV}^2$ (Fig. 5).

(iii) The pion structure function is expressed through the pion soft wave function and constituent quark structure function. By describing the data on the pion valence quark x distribution, we find the parameters of the x distribution of valence quarks inside a constituent quark to be in qualitative agreement with a Reggeized QCD-gluon

intercept calculation [18].

The paper is organized as follows.

Section II considers the pion as quark-antiquark bound state within the light-cone technique [17] reformulated as dispersion relation integrals and presents the expressions for the pion form factor and quark distribution in deep inelastic scattering. All necessary technical details relevant to the pion description are given in the Appendixes. The results are discussed in the Sec. III. A brief summary and outlook are given in the Conclusion.

II. PION FORM FACTOR AND STRUCTURE FUNCTION

The light-cone technique expressed in the form of the dispersion relation integrals [20] allows one to construct a relativistic and gauge-invariant amplitude of the interaction of a composite system with an external vector field starting with a low-energy constituent scattering amplitude (see Appendix A). Two-particle s -channel interactions are consistently taken into account both in the constituent scattering amplitude and the amplitude of interaction with an external field. In the case of a bound state, its form factor and structure function are

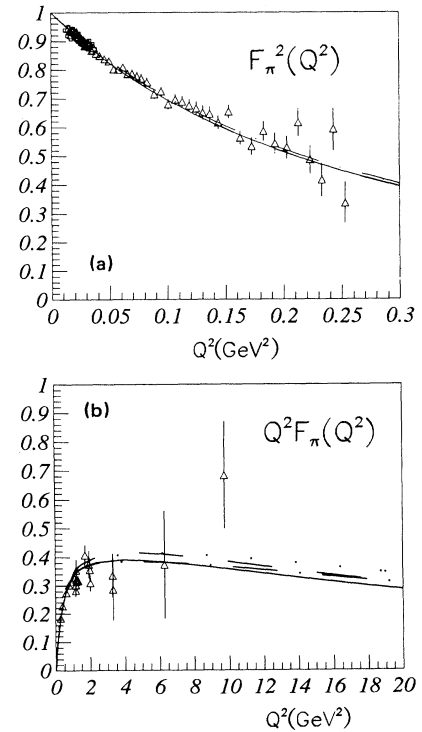


FIG. 3. The pion form factor. Solid line, calculations with the set 1 of the parameters; dashed-dotted line, set 2; dashed line, set 3; dotted line, set 4.

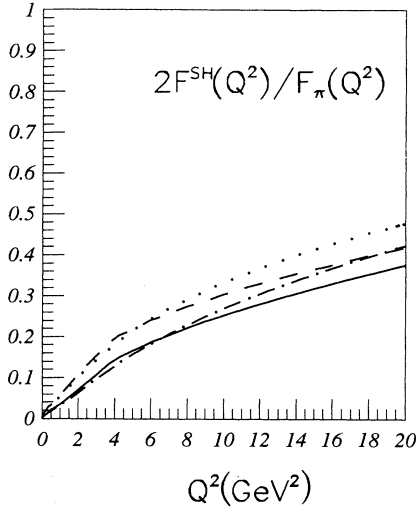


FIG. 4. The contribution of the soft-hard term to the pion form factor. The curve notation is the same as for the form factor.

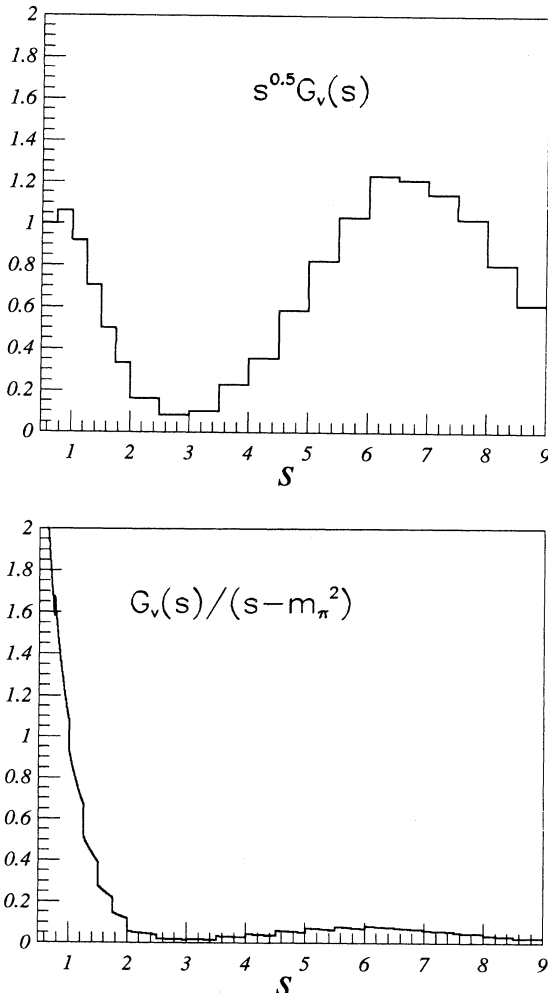


FIG. 5. The soft light-cone wave function of the pion.

expressed through the form factor and structure function of mass-shell constituents and the vertex G of a constituent bound-state transition. This vertex is defined by the two-particle irreducible block of the constituent scattering amplitude. On the one hand, the dispersion integral representation turns out to be equivalent to the Bethe-Salpeter treatment with a separable kernel of a special form, the vertex G being connected with the amputated Bethe-Salpeter wave function of the bound state. On the other hand, this approach can be formulated as a light-cone description of a bound state with the special form of spin transformation (the Melosh rotation). Because of the relativistic invariance, the dispersion integral approach does not face the problem of choosing an appropriate component of the current for the form factor calculation. The function G determines the bound-state light-cone wave function [20]. Note also that only amplitudes for on-shell constituents contribute to the corresponding amplitudes of the bound state. This guarantees gauge invariance of the derived expressions and escapes the problem of constituent amplitudes off the mass shell. All relevant details can be found in Appendix A.

Our position on the pion structure completely coincides with the viewpoint formulated by Weinberg [11]: “The successes of the constituent quark model suggests that quarks may be treated much like ordinary massive hadrons, with the only difference that they are subject to color forces that become effective at large separations and keep the quarks trapped, but are otherwise quite weak. If this is so, it makes sense to ask what are the axial-vector coupling g_A and other electroweak couplings of the quarks, and use these as inputs in the quark model calculations of ordinary hadrons.”

To derive the expressions for the soft amplitudes of the pion interactions ($\langle \pi | \mu \nu \rangle$ and $\langle \pi | J_\mu | \pi \rangle$) we start with the corresponding amplitudes of the constituent quark interactions ($\langle Q \bar{Q} | \mu \nu \rangle$ and $\langle Q \bar{Q} | J_\mu | Q \bar{Q} \rangle$) and single out the pion poles. The amplitude of the $Q \bar{Q}$ interaction turns out to be the basic quantity describing the pion constituent-quark structure. Near the pion pole, the amplitude is dominated by the $J = 0$ partial wave amplitude which can be expressed in the two-particle approximation through the dispersion loop graph B_π with the vertex

$$\frac{\bar{Q}^a(P-k) i \gamma_5 Q^a(k)}{\sqrt{N_c}} G(P^2), \quad (14)$$

with a a color index, $N_c = 3$ the number of quark colors, $k^2 = m^2$, $(P-k)^2 = m^2$, m the constituent-quark mass, and $P^2 = s \neq m_\pi^2$. For on-shell constituents, the expression (14) is the only independent spinorial structure. We consider π^+ and omit the flavor which gives the unity factor.

The pionic dispersion loop graph of Fig. 6, which is connected with the pion vertex normalization, reads

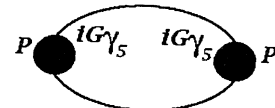


FIG. 6. Pionic dispersion loop graph $B_\pi(P^2)$.

$$B_\pi(P^2) = \int_{4m^2}^{\infty} \frac{ds G^2(s)}{\pi(s - P^2)} \rho_\pi(s), \quad B_\pi(m_\pi^2) = 1, \quad (15)$$

with $\rho_\pi(s)$ the spectral density of the Feynman loopgraph:

$$\begin{aligned} \rho_\pi(s) &= -\frac{1}{8\pi^2} \int dk_1 dk_2 \delta(k_1^2 - m^2) \delta(k_2^2 - m^2) \delta(P - k_1 - k_2) \text{Sp}((\hat{k}_1 + m) i\gamma_5 (m - \hat{k}_2) i\gamma_5) \\ &= \frac{s}{8\pi} \sqrt{1 - \frac{4m^2}{s}} \theta(s - 4m^2). \end{aligned} \quad (16)$$

Taking into account constituent-quark rescatterings leads to the renormalization of G (see Appendix A), and the soft constituent-quark structure of the pion is given by the vertex

$$\frac{\bar{Q}^a(P - k) i\gamma_5 Q^a(k)}{\sqrt{N_c}} G_v(P^2), \quad (17)$$

where $G_v(s) = G(s)/B'_\pi(m_\pi^2)$,

$$\int \frac{G_v^2(s) \rho_\pi(s) ds}{\pi(s - m_\pi^2)^2} = 1.$$

The function G_v is supposed to be nonzero at $s < s_0$ in accordance with (12). Once the soft vertex (17) is fixed, we can proceed with calculating pion interaction amplitudes.

A. Weak decay of the pion

Let us consider the decay $\pi \rightarrow \mu\nu$. The corresponding amplitude reads

$$\langle \pi^+(P_\pi) | A_\mu^{aa}(0) | 0 \rangle = i(P_\pi)_\mu f_\pi, \quad f_\pi = 130 \text{ MeV}. \quad (18)$$

To obtain the expression for this matrix element we must first consider the quantity

$$\langle U \bar{D} | A_\mu^{aa}(0) | 0 \rangle, \quad (19)$$

with U and D constituent quarks, while the axial-vector current $A_\mu(0) = \bar{u}(0) \gamma_\mu \gamma_5 d(0)$ is defined through current quarks. Next, we must single out the pole corresponding to the pion.

The *bare* matrix element reads (Q denotes a constituent quark)

$$\begin{aligned} \langle Q(k) \bar{Q}(P - k) | A_\mu^{aa}(0) | 0 \rangle_{\text{bare}} \\ = \bar{Q}(P - k) [\gamma_\mu \gamma_5 g_A^0(P^2) + P_\mu \gamma_5 h_A^0(P^2)] Q(k). \end{aligned} \quad (20)$$

If current quarks were identical to constituent ones, we would have had

$$g_A^0(P^2) \equiv 1, \quad h_A^0(P^2) \equiv 0.$$

It is reasonable to assume that at least $g_A^0(0)$ and $h_A^0(0)$ are not far from these values. The *bare* matrix element enters into a single-loop graph B_μ whose spectral density reads

$$-\frac{\sqrt{N_c}}{8\pi^2} \int dk_1 dk_2 \delta(k_1^2 - m^2) \delta(k_2^2 - m^2) \delta(P - k_1 - k_2) \text{Sp}([\gamma_\mu \gamma_5 g_A^0(P^2) + P_\mu \gamma_5 h_A^0(P^2)] (\hat{k}_1 + m) i\gamma_5 (m - \hat{k}_2)). \quad (21)$$

So the loop graph is equal to

$$B_\mu = iP_\mu \left[4m g_A^0(P^2) - \frac{P^2}{2} h_A^0(P^2) \right] \sqrt{N_c} \int \frac{ds G(s)}{\pi(s - M^2)} \frac{1}{16\pi} \sqrt{1 - 4m^2/s}. \quad (22)$$

After allowing for constituent-quark rescatterings we come to the series of dispersion graphs of Fig. 7 which gives

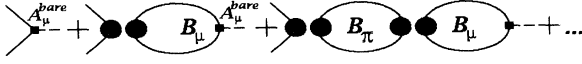
$$\langle Q(k) \bar{Q}(P - k) | A_\mu^{aa}(0) | 0 \rangle = \bar{Q}(P - k) [\gamma_\mu \gamma_5 g_A(P^2) + P_\mu \gamma_5 h_A(P^2)] Q(k), \quad (23)$$

with

$$\begin{aligned} g_A(P^2) &= g_A^0(P^2), \\ h_A(P^2) &= h_A^0(P^2) - \frac{G(P^2)}{1 - B_\pi(P^2)} 4m \left[g_A^0(P^2) - \frac{P^2}{2m} h_A^0(P^2) \right] \int \frac{ds G(s)}{\pi(s - M^2)} \frac{1}{16\pi} \sqrt{1 - 4m^2/s}. \end{aligned}$$

The form factor h_A develops a pole at $P^2 = m_\pi^2$ as $B_\pi(m_\pi^2) = 1$. Near $P^2 = m_\pi^2$ one has

$$\langle \bar{Q} Q | A_\mu | 0 \rangle = \langle \bar{Q} Q | \pi \rangle \frac{1}{m_\pi^2 - P^2} \langle \pi | A_\mu | 0 \rangle. \quad (24)$$

FIG. 7. The series of dispersion graphs for $\langle Q\bar{Q}|A_\mu(0)|0\rangle$.

Comparing the pole terms in (34) and (35) and using the relation

$$\langle \pi | Q\bar{Q} \rangle = \frac{\bar{Q}i\gamma_5 Q}{\sqrt{N_c}} G_v,$$

one finds

$$\begin{aligned} \langle \pi | A_\mu^{aa}(0) | 0 \rangle &= iP_\mu 4m [g_A^0(m_\pi^2) - \frac{m_\pi^2}{2m} h_A^0(m_\pi^2)] \sqrt{N_c} \\ &\times \int \frac{ds G_v(s)}{\pi(s-M^2)} \frac{1}{16\pi} \sqrt{1-4m^2/s} = iP_\mu f_\pi \end{aligned} \quad (25)$$

and hence

$$4m\kappa\sqrt{N_c} \int \frac{ds G_v(s)}{\pi(s-M^2)} \frac{1}{16\pi} \sqrt{1-4m^2/s} = f_\pi, \quad (26)$$

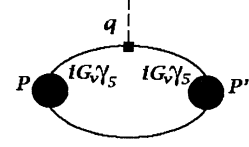
with

$$\kappa = g_A^0(m_\pi^2) - \frac{m_\pi^2}{2m} h_A^0(m_\pi^2). \quad (27)$$

We can neglect the second term because the small value h_A^0 is further suppressed by m_π^2 . Finally, one finds

$$\kappa \approx g_A^0(m_\pi^2) \approx g_A^0(0) \equiv g_A, \quad (28)$$

where g_A is the constituent-quark axial-vector coupling constant. From the analysis of the neutron β decay within various models, the value of g_A was found to be

FIG. 8. The soft-soft contribution $F_\pi^{SS}(q^2)$ to pion form factor.

in the range from 0.75 (nonrelativistic constituent-quark model without configuration mixing in the nucleon wave function, $m \approx 0.33$ GeV) up to 1.0 (relativistic quark model with light constituent quarks, $m \approx 0.25$ GeV [15].) Here we use relation (28) to fix the value of g_A related to a particular pion wave function such that (41) reproduces the observed value $f_\pi = 130$ MeV. The value of g_A is found to lie in the range $g_A \approx 0.75$ –1 (see Table I).

B. Soft-soft contribution to pion form factor

The form factor of a pion is given by the matrix element

$$\langle P'_\pi | J_\mu^{em}(0) | P_\pi \rangle = (P'_\pi + P_\pi)_\mu F_\pi(q^2), \quad (29)$$

$$P_\pi^2 = P'^2_\pi = M^2, \quad (P'_\pi - P_\pi)^2 = q^2.$$

The double dispersion representation for the soft-soft form factor corresponds to Fig. 8:

$$F_\pi^{SS}(q^2) = \int \frac{ds G_v(s)}{\pi(s-M^2)} \frac{ds' G_v(s')}{\pi(s'-M^2)} \Delta_\pi(s', s, q^2) f_c(q^2). \quad (30)$$

Here f_c is a constituent form factor, $f_c(0) = 1$, and Δ_π is defined as

$$\begin{aligned} &-\frac{1}{8\pi} \int dk_1 dk'_1 dk_2 \delta(k_1^2 - m^2) \delta(k'_1{}^2 - m^2) \delta(k_2^2 - m^2) \delta(P - k_1 - k_2) \delta(P' - k'_1 - k_2) \\ &\times \text{Sp}((\hat{k}'_1 + m) \gamma_\mu (\hat{k}_1 + m) i\gamma_5 (m - \hat{k}_2) i\gamma_5) = 2P_\mu(q) \Delta_\pi(s', s, q^2), \end{aligned} \quad (31)$$

with

$$P_\mu(q) = \left(P - \frac{qP}{q^2} \right)_\mu, \quad P^2 = s, \quad P'^2 = s', \quad (P' - P)^2 = q^2.$$

The trace reads

$$\frac{1}{4} \text{Sp}((\hat{k}'_1 + m) \gamma_\mu (\hat{k}_1 + m) \gamma_5 (m - \hat{k}_2) \gamma_5) = m^2(k_1 + k'_1)_\mu + k_{1\mu}(k'_1 k_2) + k'_{1\mu}(k_1 k_2) - k_{2\mu}(q k_1). \quad (32)$$

Multiplying both sides of (31) by P_μ and using (32) one obtains

$$\Delta_\pi(s', s, q^2) = \frac{-q^2 s s'}{4\lambda^{3/2}(s', s, q^2)} \theta(-q^2 s' s - m^2 \lambda(s', s, q^2)), \quad q^2 < 0, \quad (33)$$

with $\lambda(s', s, q^2) = (s' + s - q^2)^2 - 4s's$. At $q^2 = 0$ one finds

$$\Delta_\pi(s', s, q^2 = 0) = \frac{s}{8} \sqrt{1 - \frac{4m^2}{s}} \delta(s' - s) = \pi \rho_\pi(s) \delta(s' - s) \quad (34)$$

and

$$F_\pi^{\text{SS}}(0) = f_c(0) \int \frac{ds G_v^2(s)}{\pi(s - m_\pi^2)^2} \rho_\pi(s) = 1. \quad (35)$$

As we have pointed out in Appendix A, this is just the Ward identity consequence.

To reveal the relationship between the dispersion integral (30) and the light-cone technique, we introduce the light-cone variables

$$k_- = \frac{1}{\sqrt{2}}(k_0 - k_z), \quad k_+ = \frac{1}{\sqrt{2}}(k_0 + k_z), \quad k^2 = 2k_+k_- - k_\perp^2 \quad (36)$$

into the integral representation for the form factor spectral density (31). Performing k_- integration and setting ($\mu = +$) in both sides of (32) one finds

$$\Delta_\pi(s', s, q^2) = \frac{1}{16\pi} \int \frac{dx d^2k_\perp}{x(1-x)^2} \delta\left(s - \frac{m^2 + k_\perp^2}{x(1-x)}\right) \delta\left(s' - \frac{m^2 + (k_\perp - xq_\perp)^2}{x(1-x)}\right) [(s' + s)(1-x) + q^2x]. \quad (37)$$

Here we denoted $x = k_{2+}/P_+$ and $k_\perp = k_{2\perp}$.

Substituting (37) into (30) and performing s and s' integrations, one derives

$$F_\pi^{\text{SS}}(q_\perp^2) = \frac{1}{\pi} \int dx d^2k_\perp \psi(x, k_\perp) \psi(x, k_\perp - xq_\perp) \beta(x, k_\perp, q_\perp) f_c(q_\perp^2), \quad (38)$$

where the radial light-cone wave function of a pion is introduced:

$$\psi(x, k_\perp) = \frac{G_v(s) \sqrt{s}}{\pi \sqrt{8(s - m_\pi^2)} \sqrt{x(1-x)}}, \quad s = \frac{m^2 + k_\perp^2}{x(1-x)}, \quad (39)$$

$$\beta = \frac{m^2 + k_\perp^2 - xk_\perp q_\perp}{\sqrt{m^2 + k_\perp^2} \sqrt{m^2 + (k_\perp - xq_\perp)^2}}, \quad \beta(q_\perp = 0) = 1.$$

The quantity β accounts for the contribution of spins. It is different from unity at $q_\perp \neq 0$ because both the spin-nonflip and spin-flip amplitudes of the interacting quark contribute. Equation (35) is the normalization condition for the soft radial wave function:

$$\int dx dk_\perp^2 |\psi(x, k_\perp)|^2 = 1. \quad (40)$$

In terms of this wave function, the pion axial-vector decay constant f_π decay is represented as

$$g_A \frac{\sqrt{N_c}}{\sqrt{2\pi}} \int dx dk_\perp^2 \frac{m}{\sqrt{m^2 + k_\perp^2}} \psi(x, k_\perp) = f_\pi. \quad (41)$$

The same expressions for the form factor and pion electroweak constant as (38)–(41) were derived in Refs. [14–16]. In contrast with these papers where such formulas were applied to describing the total pion form factor, we use them for calculating the soft-soft contribution.

The soft-soft form factor involves the constituent-quark form factor which should satisfy the conditions $f_c(0) = 1$ and $f_c(Q^2) \rightarrow S(Q^2)$ at large $Q^2 = -q^2$. Here $S(Q^2)$ is the Sudakov form factor which is taken in the form [8]

$$S(Q^2) = \exp \left[-\frac{\alpha_s(Q^2)}{2\pi} C_F \ln^2 \left(\frac{Q^2}{Q_0^2} \right) \right], \quad (42)$$

$$C_F = \frac{N_c^2 - 1}{2N_c} = \frac{4}{3}, \quad Q_0 \approx 0.85\text{--}1 \text{ GeV},$$

with α_s the coupling constant. At low Q^2 we assume α_s to be frozen at 1 GeV²: Namely, we set

$$\alpha_s(Q^2) = \begin{cases} \frac{4\pi}{9} \ln^{-1} \left(\frac{Q^2}{\Lambda^2} \right), & \Lambda = 0.22 \text{ GeV}, \\ Q^2 < 1 \text{ GeV}^2, \\ \text{const}, & Q^2 < 1 \text{ GeV}^2. \end{cases} \quad (43)$$

The constituent-quark form factor is taken as

$$f_c(Q^2) = \begin{cases} 1, & Q < Q_0, \\ S(Q^2), & Q > Q_0, \end{cases} \quad S(Q_0^2) = 1. \quad (44)$$

Note that the Sudakov suppression is absent in the soft-hard term.

C. Soft-hard contribution to the pion form factor

In accordance with (10), the soft-hard contribution is described by the two graphs of Fig. 2(b) or Fig. 9, with one-gluon exchanges.

The corresponding soft-hard form factor F_π^{SH} , accounts for the assumption that at $s'' > s_0$ the $\bar{Q}Q$ interaction is described by the convolution of the one-gluon exchange kernel with the soft-region vertex G_v (the right block in Fig. 9).

The dispersion relation integral for the F_π^{SH} reads

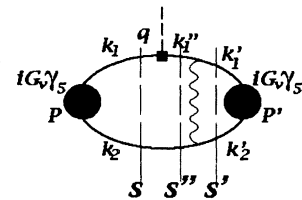


FIG. 9. The soft-hard contribution F_π^{SH} to pion form factor.

$$F^{\text{SH}} = \int \frac{ds G_v(s) \theta(s < s_0)}{\pi(s - m_\pi^2)} \frac{ds'' \theta(s'' > s_0)}{\pi(s'' - m_\pi^2)} D(s, s'', s', q^2) \frac{ds' G_v(s') \theta(s' < s_0)}{\pi(s' - m_\pi^2)}. \quad (45)$$

In this expression, $D(s, s'', s', q^2)$ is a spectral density which takes into account the one-gluon exchange at large s'' . To derive the spectral density of F^{SH} , we start with the corresponding Feynman graph with pointlike vertices:

$$\begin{aligned} 2P_\mu(q) F^{\text{SH}}(q^2) &= \frac{\text{Sp}(\lambda^A \lambda^A)}{4N_c} g^2 \int \frac{dk}{(2\pi)^4 i} \frac{dk'}{(2\pi)^4 i} \\ &\times \frac{1}{m^2 - k^2} \frac{1}{m^2 - (P - k)^2} \frac{1}{m^2 - (P' - k)^2} \frac{1}{m^2 - k'^2} \frac{1}{m^2 - (P' - k')^2} \frac{1}{m_G^2 - (k' - k)^2} \\ &\times \text{Sp}((\hat{k}_1 + \hat{q} + m)\gamma_\mu(\hat{k}_1 + m)i\gamma_5(m - \hat{k}_2)\gamma_\alpha(m - \hat{k}_2')i\gamma_5(\hat{k}_1' + m)\gamma^\alpha). \end{aligned} \quad (46)$$

In (46) m_G is the gluon mass which depends on the gluon momentum squared $-(k' - k)^2$ and is normalized to be of the order of 1 GeV in the soft region [21]. To allow only for two-particle intermediate states we consider the contribution of s , s'' , and s' cuts and neglect the contribution of three-particle intermediate states with cutting the gluon line: Three-particle states are beyond the scope of our consideration. The resulting spectral density over both soft s and s' reads

$$\begin{aligned} \Delta^{\text{SH}}(s', s, q^2) &= \theta(s < s_0)\theta(s' < s_0) g^2 C_F \int \frac{ds''}{s'' - m_\pi^2} \theta(s'' > s_0) \text{Tr}(s, s', s'', q^2) \\ &\times \int \frac{dk_1 dk_2 dk_1''}{8\pi^2} \delta(k_1^2 - m^2) \delta(k_2^2 - m^2) \delta(k_1''^2 - m^2) \delta(P - k_1 - k_2) \delta(P'' - k_1'' - k_2) \delta(k_1'' - k_1 - q) \\ &\times \int \frac{dk_1' dk_2'}{8\pi^2} \delta(k_1'^2 - m^2) \delta(k_2'^2 - m^2) \delta(P' - k_1' - k_2') \frac{1}{m_G^2 - (k_2 - k_2')^2}, \end{aligned} \quad (47)$$

with $P^2 = s$, $P''^2 = s''$, $P'^2 = s'$.

The quantity $\text{Tr}(s, s', s'', q^2)$ is the dispersion expression for the fermion-loop trace with all fermions taken on mass shell (for details see Appendix B):

$$\begin{aligned} \text{Sp}((\hat{k}_1 + \hat{q} + m)\gamma_\mu(\hat{k}_1 + m)i\gamma_5(m - \hat{k}_2)\gamma_\alpha(m - \hat{k}_2')i\gamma_5(\hat{k}_1' + m)\gamma^\alpha) &= 2P_\mu(q) \text{Tr}, \\ \text{Tr} = 2s' (\alpha(s'', s, q^2)(s'' + s - q^2) + q^2) - 4m^2 [\alpha(s'', s, q^2)(s' + s - q^2) + q^2], \end{aligned} \quad (48)$$

where

$$\alpha(s'', s, q^2) = \frac{-q^2(s'' + s - q^2)}{(s'' - s)^2 - 2q^2(s'' + s) + q^4}$$

and

$$s = \frac{m^2 + k_\perp^2}{x(1-x)}, \quad s'' = \frac{m^2 + (k_\perp - xq_\perp)^2}{x(1-x)}, \quad s' = \frac{m^2 + (k'_\perp - x'q_\perp)^2}{x'(1-x')}.$$

Use again the light-cone variables (36). Performing k_- integration and denoting $k = k_2$, $k' = k'_2$, $x = k_{2+}/P_+$, $x' = k'_{2+}/P_+$, $k_\perp = k_{2\perp}$, $k'_\perp = k'_{2\perp}$ we come to the final expression

$$\begin{aligned} F^{\text{SH}}(q_\perp^2) &= 4\pi C_F \int \frac{dx d^2 k_\perp}{16\pi^3 x(1-x)^2} \frac{G_v(s) \theta(s < s_0)}{\frac{m^2 + k_\perp^2}{x(1-x)} - m_\pi^2} \frac{\theta(s'' > s_0)}{\frac{m^2 + (k_\perp - xq_\perp)^2}{x(1-x)} - m_\pi^2} \\ &\times \frac{dx' d^2 k'_\perp}{16\pi^3 x'(1-x')} \frac{G_v(s') \theta(s' < s_0)}{\frac{m^2 + (k'_\perp - x'q_\perp)^2}{x'(1-x')} - m_\pi^2} \text{Tr}(s, s', s'', q^2) \frac{\alpha_s [-(k - k')^2]}{m_G^2 - (k' - k)^2}, \end{aligned} \quad (49)$$

where

$$-(k' - k)^2 = \frac{(k'_\perp x - k_\perp x')^2 + m^2(x - x')^2}{xx'}.$$

In (49) the renormalization $g^2 \rightarrow 4\pi\alpha_s [-(k - k')^2]$ is taken into account. Introducing the light-cone radial wave function (39) in (49), we find the soft-hard form factor in the form

$$\begin{aligned} F^{\text{SH}}(q_\perp^2) &= \frac{C_F}{8\pi} \int \frac{dx d^2 k_\perp}{\pi \sqrt{m^2 + k_\perp^2} (1-x)} \psi(x, k_\perp) \theta(s < s_0) \frac{\theta(s'' > s_0)}{\frac{m^2 + (k_\perp - xq_\perp)^2}{x(1-x)} - m_\pi^2} \\ &\times \frac{dx' d^2 k'_\perp}{\sqrt{m^2 + (k'_\perp - x'q_\perp)^2}} \psi(x', k'_\perp - x'q_\perp) \theta(s' < s_0) \text{Tr}(s, s', s'', q^2) \frac{\alpha_s [-(k - k')^2]}{m_G^2 - (k' - k)^2}. \end{aligned} \quad (50)$$

One can easily see that $F^{\text{SH}}(0) = 0$.

Let us turn to the region of large Q^2 and compare the soft-hard term which dominates the form factor with the standard PQCD expression (3) and (4). Using the relations

$$\text{Tr} \rightarrow 4m^2 Q^2 x \quad \text{and} \quad -(k'_2 - k_2)^2 \rightarrow xx' Q^2,$$

we find

$$F_\pi(Q^2) \rightarrow \frac{1}{\kappa^2} \int \phi(x, s_0) dx \frac{8\pi}{9} \frac{\alpha_s(xx' Q^2)}{xx' Q^2} \phi(x', s_0) dx'. \quad (51)$$

Here we introduced the distribution amplitude $\phi(x, s_0)$ normalized by the standard condition

$$\int \phi(x, s_0) dx = f_\pi. \quad (52)$$

This distribution amplitude is related to the soft radial wave function (39) via the relation

$$\begin{aligned} \phi(x, s_0) &= 4m\sqrt{N_c\kappa} \int \frac{ds G_v(s)}{16\pi^2(s - m_\pi^2)} \theta\left(\frac{m^2}{x(1-x)} < s\right) \theta(s < s_0) \\ &= \frac{\sqrt{N_c\kappa}}{\sqrt{2\pi}} \int dk_\perp^2 \frac{m}{\sqrt{m^2 + k_\perp^2}} \psi(x, k_\perp) \theta\left(\frac{m^2 + k_\perp^2}{x(1-x)} < s_0\right). \end{aligned} \quad (53)$$

The expression (51) differs from (8) by the factor $1/\kappa^2$. If we identify constituent quarks with bare PQCD quarks, then $\kappa = g_A^0 = 1$. Here we assume such an identification to be not well justified in the region $Q^2 \leq 10 \text{ GeV}^2$ and hence we allow κ to be in the range from 0.75 to 1.

Actually, a constituent quark is a Fock state involving the components $q_{\text{val}}, q_{\text{val}}\bar{q}q, q_{\text{val}}\bar{q}qg, \dots$. At asymptotically large momentum transfers only the valence component survives whereas all other components do not contribute to the form factor. The problem of the typical Q at which the transfer to the asymptotic regime occurs is still opened. It is quite natural that the expression (51) gives a larger value for the form factor at $\kappa < 1$ since it includes the contribution of all higher Fock components of the constituent quark in addition to the valence one.

D. Structure function

Now we have all that is necessary to calculate the pion structure function $F_2(x)$. This function is given by the convolution of the pion light-cone soft wave function and the corresponding constituent-quark structure function $f_2^j(x)$:

$$F_2(x, Q^2) = \sum_{j=Q, \bar{Q}} \int_x^1 dk_\perp^2 dx' \psi(x', k_\perp)^2 f_2^j\left(\frac{x}{x'}, Q^2\right). \quad (54)$$

The leading order expressions for these structure functions in terms of parton densities read

$$F_2(x) = \sum_{\text{flavors}} e_i^2 x Q_i(x), \quad f_2^j(x) = \sum_{\text{flavors}} e_i^2 x q_i^j(x), \quad (55)$$

where Q_i and q_i^j are quark parton densities of a given flavor i inside a pion and constituent quark j , respectively.

At large x the behavior of the structure functions is

determined by the valence quark (antiquark) distribution $v(x)$ inside the constituent quark (antiquark). The latter is taken in the form

$$v(x) \approx x^{-a}(1-x)^{-b} [1 - N(1-x)^c]. \quad (56)$$

The parameters in this formula are chosen such that $v(x)$ should satisfy the following sum rules at $Q_0^2 = 10 \text{ GeV}^2$:

$$\int_0^1 v(x, Q_0^2) dx = 1, \quad \int_0^1 v(x, Q_0^2) x dx = 0.35. \quad (57)$$

The last number is the fraction of constituent-quark momentum carried by the valence quark. Because of the sum rule for momentum, this value is equal to the fraction of hadron momentum carried by valence quarks. For a proton this fraction is known to be ≈ 0.35 at 10 GeV^2 .

III. RESULTS OF FITTING THE DATA ON THE FORM FACTOR AND DEEP INELASTIC PARTON DISTRIBUTION

Figure 3 shows the results of fitting the data on $F_\pi(Q^2)$ [22] via the formulas (38) and (39) for F^{SS} and (50) for F^{SH} . Figure 3(a) demonstrates the region of low Q^2 where F^{SS} dominates; Fig. 3(b) emphasizes the region of moderately large Q^2 , $Q^2 = 5\text{--}20 \text{ GeV}^2$. Figure 4 plots the typical contribution of the soft-hard term to the pion form factor. Several variants of the calculation relate to different sets of the parameters m_G , α_s , and m presented in Table I. Let us point out that g_A^0 calculated with the determined wave function appreciably depends on the constituent-quark mass: For a heavy constituent quark g_A^0 is rather small and equal to 0.86, whereas for a light constituent quark g_A^0 is close to unity.

In all the fits the soft pion wave function $\psi(x, k_\perp^2)$ was the basic variational quantity. Figure 5 and Table II present the typical reconstructed soft wave function. A specific feature of the reconstructed wave function is the quasizone character of $\bar{q}q$ excitations in the pion. We

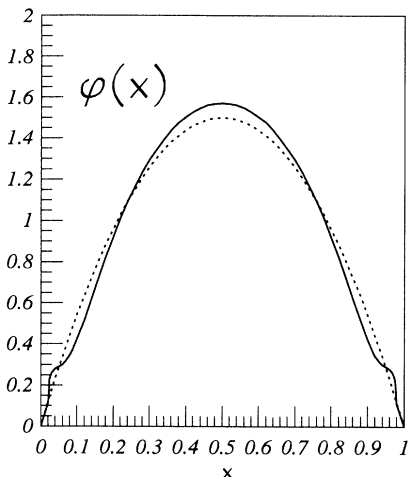


FIG. 10. The distribution amplitude. Solid line, our calculation; dashed line, asymptotical curve $\phi(x) = 6x(1-x)$.

tried to find a parametrization without a dip in the region 2–4 GeV² but failed; all the used fitting procedures suggested qualitatively similar double-humped wave functions. So one can think this dip reflects some essential feature of the $\bar{q}q$ dynamics inside the pion. However, we have no definite ideas on the origin of such a specific behavior.

Figure 10 displays the distribution amplitude $\phi(x)$ calculated with the determined $G_v(s)$. It turned out to be very close to the asymptotic function (7).

Figure 11 presents the valence-quark distribution inside the pion. The parameters of the distribution (56), $b = 0.99$ and a and c from the range $a = 0.5$ – 0.7 and $c = 1$ – 2 , were found to provide a reasonable description of the data [23]. If the valence-quark distribution is determined by the Reggeized-gluon exchange, then our result gives for its intercept (b) a value close to unity in qualitative agreement with [18].

IV. CONCLUSION

We have analyzed the pion structure within a dispersion relation formulation of the light-cone technique when the pion in the soft region is treated as a two-constituent-quark bound state. At small values of the $\bar{q}q$ light-cone energy the pion is described by a model soft wave function, whereas at large values the one-gluon hard exchange is taken into account. This provides the form factor high- Q^2 asymptotic behavior in agreement with PQCD. The obtained pion form factor describes well the available ex-

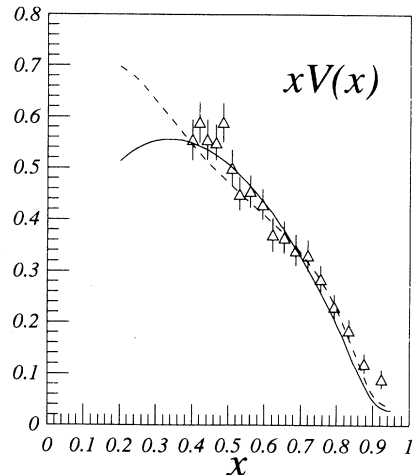


FIG. 11. Valence distribution in a pion $xV(x, Q^2 = 10 \text{ GeV}^2)$. Solid curve, $a = 0.69$, $b = 0.99$, $c = 1$; dashed curve, $a = 0.46$, $b = 0.99$, $c = 1.55$.

perimental data at $Q^2 \leq 10 \text{ GeV}^2$.

Our results are as follows.

(1) We considered the soft-soft (F^{SS}) and soft-hard ($2F^{\text{SH}}$) contributions to the pion form factor within light-cone quantum mechanics. The derived expressions involve the soft radial wave function of the pion which has been treated as a variational parameter of the approach. By fitting the data on the pion form factor at $Q^2 \leq 3 \text{ GeV}^2$, we determined this soft radial wave function. This allowed a calculation of the relative soft-hard contribution to the pion form factor in a broad range of momentum transfers. It turned out to be relatively small (less than 50% at $Q^2 = 20 \text{ GeV}^2$) because we used a large value for the boundary of the light-cone energy squared dividing the soft and the hard regions ($s_0 = 9 \text{ GeV}^2$) and hence we related a large portion of the pion form factor to the soft-soft contribution. However, smaller values of this boundary do not change qualitatively the results, except for quantitatively increasing the soft-hard fraction.

The calculated pion axial-vector decay constant agrees well with the experimental value.

(2) The soft radial light-cone wave function as a function of the square of the light-cone $\bar{q}q$ energy s has been found to demonstrate a specific behavior: It is large at $s \leq 2 \text{ GeV}^2$, close to zero as $s = 2$ – 4 GeV^2 , and has a bump in the region $s = 4$ – 9 GeV^2 . Our attempts to find a wave function of a more regular shape failed as all the fits suggested a double-humped behavior. We have no definite ideas about the origin of such a quasizone character

TABLE I. Parameters in the pion form factor calculations. We assumed $m_G(\kappa^2) = m_G^0(1 - \kappa^2/0.5)$ as $\kappa^2 < 0.5 \text{ GeV}^2$ and $m_G = 0$ as $\kappa^2 > 0.5 \text{ GeV}^2$, where κ is the gluon momentum.

	Set 1	Set 2	Set 3	Set 4
Constituent quark mass m (GeV)	0.35	0.35	0.35	0.35
m_G^0 (GeV)	0.7	0.7	0	0
α_s in (50)	$\alpha_s(Q^2/4)$	$\alpha_s(\kappa^2)$	$\alpha_s(Q^2/4)$	$\alpha_s(\kappa^2)$
$g_A(0)$	0.86	0.86	0.86	0.86

TABLE II. A step-function approximation for the soft pion vertex at $s(i) < s < s(i+1)$, $G_v(s)s^{0.5}=C_i$.

$s(i)$ (GeV ²)	$4m^2$	0.75	1.0	1.25	1.5	1.75	2.0	2.5	3.0	3.5	4.0
C_i	1.00	1.06	0.92	0.71	0.50	0.33	0.16	0.08	0.10	0.23	0.36
$s(i)$ (GeV ²)	4.5	5.0	5.5	6.0	6.5	7.0	7.5	8.0	8.5	9.0	∞
C_i	0.59	0.82	1.03	1.23	1.21	1.14	1.02	0.80	0.61	0	

of the $\bar{q}q$ excitations. Nevertheless, such an unexpected wave function seems to reflect some unknown essential details of the quark dynamics in the pion.

(3) The distribution amplitude $\phi(x)$ calculated with the obtained soft wave function turns out to be very close to the asymptotic function $\phi_\pi^{\text{as}}(x)$ predicted by PQCD.

(4) Describing the data on deep inelastic scattering off the pion allowed investigating the parton structure of the constituent quark. The distribution of the valence-quark parton in the constituent quark is found to be in a qualitative agreement with the parametrization suggested by the Reggeized-gluon exchange.

ACKNOWLEDGMENTS

The authors are grateful to the International Science Foundation for financial support under Grant No. R1000.

APPENDIX A: BOUND-STATE DESCRIPTION WITHIN DISPERSION RELATIONS

To illustrate main points of the dispersion approach we consider the case of two spinless constituents with the masses m interacting via exchanges of a meson with the mass μ . We start with the scattering amplitude

$$A(s, t) = \langle k'_1, k'_2 | S | k_1, k_2 \rangle, \quad (A1)$$

$$s = (k_1 + k_2)^2, \quad t = (k_1 - k'_1)^2.$$

The amplitude as a function of s has the threshold singularities in the complex s plane connected with elastic rescatterings of the constituents and production of new mesons at

$$s = 4m^2, (2m + \mu)^2, (2m + 2\mu)^2, \dots \quad (A2)$$

We assume that an S -wave bound state with the mass $M < 2m$ exists; then the partial amplitude $A_0(s)$ has a pole at $s = M^2$. The amplitude $A(s, t)$ has also t -channel singularities at $t = (n\mu)^2$, $n = 1, 2, 3, \dots$, connected with meson exchanges. If one needs to construct the amplitude in the low-energy region $s \geq 4m^2$, the dispersion N/D representation turns out to be convenient. Consider the S -wave partial amplitude

$$A_0(s) = \int_{-1}^1 dz A(s, t(s, z)), \quad (A3)$$

where $t(z) = -2(s/4 - m^2)(1 - z)$ and $z = \cos \theta$ in the c.m. system (c.m.s.). The $A_0(s)$ as a function of complex s has the right-hand singularities related to s -channel singularities of $A(s, t)$. In addition, it has left-

hand singularities located at $s = 4m^2 - (n\mu)^2$, $n = 1, 2, 3, \dots$. They come from t -channel singularities of $A(s, t)$. The unitarity condition in the region $s \approx 4m^2$ reads

$$\text{Im } A_0(s) = \rho(s) |A_0(s)|^2, \quad \rho(s) = \frac{1}{16\pi} \sqrt{1 - \frac{4m^2}{s}}, \quad (A4)$$

with $\rho(s)$ the two-particle phase space. The N/D method represents the partial amplitude as $A_0(s) = N(s)/D(s)$, where the function N has only left-hand singularities and D has only right-hand ones. The unitarity condition yields

$$D(s) = 1 - \int_{4m^2}^{\infty} \frac{d\tilde{s}}{\pi} \frac{\rho(\tilde{s})N(\tilde{s})}{\tilde{s} - s} \equiv 1 - B(s). \quad (A5)$$

Assuming the function N to be positive we introduce $G(s) = \sqrt{N(s)}$. Then the partial amplitude takes the form

$$A_0(s) = G(s) [1 + B(s) + B^2(s) + B^3(s) + \dots] G(s) = \frac{G(s)G(s)}{1 - B(s)}. \quad (A6)$$

This expression can be interpreted as a series of loop diagrams of Fig. 12 with the basic loop diagram

$$B(s) = \int_{4m^2}^{\infty} \frac{d\tilde{s}}{\pi} \frac{\rho(\tilde{s}) G^2(\tilde{s})}{\tilde{s} - s}. \quad (A7)$$

The bound state with the mass M relates to a pole both in the total and partial amplitudes at $s = M^2$, and so $B(M^2) = 1$. Near the pole one has, for the total amplitude,

$$A = \langle k'_1, k'_2 | P \rangle \frac{1}{M^2 - P^2} \langle P | k_1, k_2 \rangle + \text{regular terms} \\ \equiv \chi_P^*(k'_1, k'_2) \frac{1}{M^2 - P^2} \chi_P(k_1, k_2) + \dots, \quad (A8)$$

where $\chi_P(k_1, k_2)$ is the amputated Bethe-Salpeter amplitude of the bound state. The dispersion amplitude near the pole reads

$$A = N/D + \text{regular terms related to other partial waves} \\ = \frac{G^2(M^2)}{(M^2 - s)B'(M^2)} + \dots \equiv \frac{G_v^2(M^2)}{M^2 - s} + \dots, \quad (A9)$$

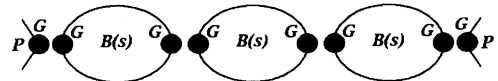


FIG. 12. One of the terms in the expansion of $A_0(s)$.

where G_v is a vertex of the bound-state transition to the constituents. The singular terms correspond to each other and hence

$$\chi_P(k_1, k_2) \rightarrow G_v(P^2) \equiv \frac{G(P^2)}{\sqrt{B'(M^2)}}. \quad (\text{A10})$$

$$\begin{aligned} T_\mu &= \langle k'_1, k'_2 | P' \rangle \frac{1}{P'^2 - M^2} \langle P' | J_\mu(q) | P \rangle \frac{1}{P^2 - M^2} \langle P | k_1, k_2 \rangle + \dots \\ &= \chi_P^*(k'_1, k'_2) \frac{1}{P'^2 - M^2} (P' + P)_\mu F(q^2) \frac{1}{P^2 - M^2} \chi_P(k_1, k_2) + \dots, \end{aligned} \quad (\text{A11})$$

where the bound-state form factor is defined as

$$\langle P' | J_\mu(q) | P \rangle = (P' + P)_\mu F(q^2). \quad (\text{A12})$$

The dispersion amplitude T_μ with only two-particle singularities in the P^2 and P'^2 channels taken into account is given [19] by the series of graphs in Fig. 13.

These graphs are obtained from the dispersion scattering amplitude series by inserting a photon line into constituent lines. The amplitude reads

$$T_\mu(P', P, q) = 2P_\mu(q)T(s', s, q^2) + \frac{q_\mu}{q^2}C, \quad (\text{A13})$$

$$P^2 = s, \quad P'^2 = s', \quad q = P' - P,$$

$$P_\mu(q) = \left(P - \frac{qP}{q^2} q \right)_\mu.$$

The dispersion method allows one to determine $T(s, s', q^2)$, which is the part of the amplitude transverse with respect to q_μ . Summing up the series of dispersion graphs in Fig. 13 gives

$$T(s', s, q^2) = \frac{G(s)}{1 - B(s)} \Gamma(s', s, q^2) \frac{G(s')}{1 - B(s')}. \quad (\text{A14})$$

Here

$$\Gamma(s', s, q^2) = \int \frac{d\tilde{s} G(\tilde{s})}{\pi(\tilde{s} - s)} \frac{d\tilde{s}' G(\tilde{s}')}{\pi(\tilde{s}' - s')} \Delta(\tilde{s}', \tilde{s}, q^2)$$

and $\Delta(\tilde{s}', \tilde{s}, q^2)$ is the double spectral density of the three-point Feynman graph with a pointlike vertex of the constituent interaction.

The longitudinal part C is given by the Ward identity

$$C = \frac{G(s)}{1 - B(s)} [B(s') - B(s)] \frac{G(s')}{1 - B(s')}. \quad (\text{A15})$$

At $s = s' = M^2$, the quantity T_μ develops both s and s' poles, and so

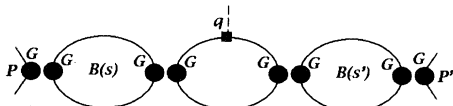


FIG. 13. One of the terms in the series for T_μ .

Emphasize that among right-hand singularities the constructed dispersion amplitude takes into account only the two-particle cut.

Let us turn to the interaction of the two-constituent system with an external electromagnetic field. The amplitude of this process, $T_\mu = \langle k'_1, k'_2 | J_\mu(q) | k_1, k_2 \rangle$, in the case of a bound state takes the form

$$\begin{aligned} T_\mu(P', P, q) &= \frac{G_v(M^2)}{M^2 - s} (P' + P)_\mu F(q^2) \frac{G_v(M^2)}{M^2 - s'} \\ &\quad + \text{less singular terms,} \end{aligned} \quad (\text{A16})$$

where

$$F(q^2) = \int \frac{ds G_v(s)}{\pi(s - M^2)} \frac{ds' G_v(s')}{\pi(s' - M^2)} \Delta(s', s, q^2) \quad (\text{A17})$$

is the bound-state form factor [see (A10) and (A11)]. So the quantity $\langle P' | J_\mu(q) | P \rangle$ corresponds to the three-point dispersion graph with the vertices G_v . The following relation is valid: $\Delta(s', s, 0) = \pi \delta(s' - s) \rho(s)$. This is a consequence of the Ward identity which relates the three-point graph at zero momentum transfer to the loop graph. This relation yields the charge normalization $F(0) = 1$. Expression (A17) gives the form factor in terms of the N function of the constituent scattering amplitude and double spectral density of the Feynman graph. In general, the following prescription works: To obtain the dispersion expression spectral density in channels corresponding to a bound state, one should calculate the related Feynman graph spectral density and multiply it by G_v .

If the constituent is a nonpoint particle, expression (A17) should be multiplied by form factor of an on-shell constituent.

APPENDIX B: TRACE CALCULATION IN THE SOFT-HARD CONTRIBUTION

The soft-hard contribution is described by a two-loop graph, and the dispersion technique prescribes that the total momenta squared of the $\bar{Q}Q$ pair should be taken different for each loop, and then the integration over these values should be performed. So we must first make the Fierz rearrangements to obtain trace calculations related to different loops. Namely, we group the expressions as follows:

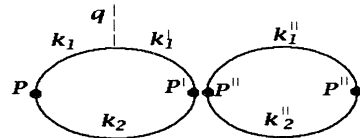


FIG. 14. Two loops in F^{SH} : momentum notation.

$$\begin{aligned}
2P_\mu(q)\text{Tr} &\equiv \text{Sp}((\hat{k}_1'' + m)\gamma_\mu(\hat{k}_1 + m)i\gamma_5(m - \hat{k}_2)\gamma_\alpha(m - \hat{k}_2')i\gamma_5(\hat{k}_1' + m)\gamma^\alpha) \\
&= \text{Sp}[(\hat{k}_1'' + m)\gamma_\mu(\hat{k}_1 + m)i\gamma_5(m - \hat{k}_2)]\gamma_\alpha[(m - \hat{k}_2')i\gamma_5(\hat{k}_1' + m)]\gamma^\alpha \\
&= \sum_{i=S,V,T,A,P} C_i \times \text{Sp}[(\hat{k}_1'' + m)\gamma_\mu(\hat{k}_1 + m)i\gamma_5(m - \hat{k}_2)O_i] \text{Sp}[(m - \hat{k}_2')i\gamma_5(\hat{k}_1' + m)O_i],
\end{aligned}$$

with $C_S = 1, C_V = -\frac{1}{2}, C_A = \frac{1}{2}, C_P = -1$. The second trace is nonzero only for A and P and we find

$$\begin{aligned}
2P_\mu(q)\text{Tr} &= \frac{1}{2}\text{Sp}[(\hat{k}_1 + \hat{q} + m)\gamma_\mu(\hat{k}_1 + m)i\gamma_5(m - \hat{k}_2)\gamma_5\gamma_\alpha] \text{Sp}[(m - \hat{k}_2')i\gamma_5(\hat{k}_1' + m)\gamma_\alpha\gamma_5] \\
&\quad - \text{Sp}[(\hat{k}_1 + \hat{q} + m)\gamma_\mu(\hat{k}_1 + m)i\gamma_5(m - \hat{k}_2)\gamma_5] \text{Sp}[(m - \hat{k}_2')i\gamma_5(\hat{k}_1' + m)\gamma_5] \equiv 2P_\mu(q)(\text{Tr}_A + \text{Tr}_P).
\end{aligned}$$

Each of the expressions Tr_i ($i = A, P$) is represented as a product of two factors, related to two different loops (see Fig. 14). We must use the relations

$$k_1 + k_2 = P, P^2 = s, \quad k_1'' = k_1 + q, \quad k_1'' + k_2 = P'',$$

$$P''^2 = s''$$

for the left loop and

$$k_1' + k_2' = P', \quad P'^2 = s'$$

for the right one and set *all* the fermions on mass shell. This procedure yields

$$\text{Tr}_A = -4m^2[\alpha(s'', s, q^2)(s' + s - q^2) + q^2],$$

$$\text{Tr}_P = 2s'[\alpha(s'', s, q^2)(s'' + s - q^2) + q^2].$$

And the final result reads

$$\begin{aligned}
\text{Tr} &= \{2s'[\alpha(s'', s, q^2)(s'' + s - q^2) + q^2] \\
&\quad - 4m^2[\alpha(s'', s, q^2)(s' + s - q^2) + q^2]\}.
\end{aligned}$$

-
- [1] S.J. Brodsky and G.P. Lepage, Phys. Lett. **87B**, 359 (1979); Phys. Rev. D **22**, 2157 (1980); A.V. Efremov and A.V. Radyushkin, JETP Lett. **25**, 210 (1977); Phys. Lett. **94B**, 45 (1980); V.L. Chernyak and A.R. Zhitnitsky, Yad. Fiz. **31**, 1053 (1980).
 - [2] S.J. Brodsky and G.P. Lepage, in *Perturbative QCD*, edited by A. H. Mueller (World Scientific, Singapore, 1989), pp. 93–241.
 - [3] V.L. Chernyak and A.R. Zhitnitsky, Phys. Rep. **112**, 173 (1984).
 - [4] N. Isgur and C. Llewellyn-Smith, Phys. Lett. B **217**, 535 (1989); Nucl. Phys. B **317**, 526 (1989).
 - [5] S. Mikhailov and A. Radyushkin, Phys. Rev. D **45**, 1754 (1991).
 - [6] V. Braun and I. Halperin, Phys. Lett. B **328**, 457 (1994).
 - [7] H.-N. Li and G. Sterman, Nucl. Phys. B **382**, 129 (1992).
 - [8] A. Radyushkin, “Qualitative and quantitative aspects of the QCD theory of elastic form factors,” Report No. CEBAF-TH-93-12, 1993, (unpublished); in *Continuous Advances in QCD*, Proceedings of the Workshop, Minneapolis, Minnesota, 1994, edited by A. V. Smilga (World Scientific, Singapore, 1994); Report No. hep-ph/9406237 (unpublished).
 - [9] T. Huang and Q.-X. Shen, Z. Phys. C **50**, 139 (1991); T. Huang, B.-Q. Ma, and Q.-X. Shen, Phys. Rev. D **49**, 1490 (1993).
 - [10] H. Fritzsch, Mod. Phys. Lett. A **5**, 625 (1990); Report No. CERN-TH. 7079/1993 (unpublished).
 - [11] S. Weinberg, Phys. Rev. Lett. **65**, 1181 (1991); **67**, 3473 (1991).
 - [12] N. Isgur and G. Karl, Phys. Lett. **72B**, 109 (1977).
 - [13] Z. Dziembowski, Phys. Rev. D **37**, 778 (1988).
 - [14] W. Jaus, Phys. Rev. D **44**, 2319 (1991).
 - [15] F. Schlumpf, Phys. Rev. D **47**, 4114 (1993); **50**, 6895 (1994).
 - [16] F. Cardarelli, I. Grach, I. Narodetskii, E. Pace, G. Salme, and S. Simula, Phys. Lett. B **332**, 1 (1994).
 - [17] M.V. Terent’ev, Sov. J. Nucl. Phys. **24**, 106 (1976); V.B. Berestetskii and M.V. Terent’ev, *ibid.* **24**, 106 (1976); **25**, 347 (1977).
 - [18] L.N. Lipatov, Sov. Phys. JETP **63**, 904 (1986).
 - [19] V.V. Anisovich, M.N. Kobrinsky, D.I. Melikhov, and A.V. Sarantsev, Nucl. Phys. A **544**, 747 (1992).
 - [20] V.V. Anisovich, D.I. Melikhov, B.C. Metsch, and H.R. Petry, Nucl. Phys. A **563**, 549 (1993).
 - [21] G. Parisi and R. Petronzio, Phys. Lett. **94B**, 51 (1980); M. Consoli and J.H. Field, Phys. Rev. D **49**, 1293 (1994).
 - [22] C. Bebek *et al.*, Phys. Rev. D **13**, 25 (1976); **17**, 1693 (1978); S.R. Amendolia *et al.*, Nucl. Phys. B **277**, 168 (1986).
 - [23] J. Badier *et al.*, Z. Phys. C **18**, 281 (1983).